

Additive manufacturing of Trabecular Titanium orthopedic implants

M. Regis, E. Marin, L. Fedrizzi, and M. Pressacco

The long-term success of an orthopedic implant largely depends on the extent of its osseointegration in the surrounding bone. During recent decades, there have been several attempts to develop porous structures and coatings in order to maximize the bone ingrowth on prosthesis surfaces. Innovative additive manufacturing technologies, such as electron beam melting (EBM), which are based upon building components by adding layers of material rather than by removing material from a raw shape, can provide a breakthrough solution, both to overcome the major limitations of the actual technologies and to significantly enhance the performance of porous scaffolds. This article reviews the latest developments in EBM technology applied to the preparation of highly biocompatible porous materials such as Trabecular Titanium and the production of orthopedic prostheses with enhanced characteristics.

Introduction

Orthopedic implants such as hip, knee, and shoulder replacements are subjected to great challenges during their use:[1] Cyclic loads, sliding wear, and the human body ambient are demanding factors for the materials employed. This has allowed research for new materials with better performance to flourish over the past 50 years. One of the critical success factors for prosthetic implants is called osseointegration and is responsible for long-term implant fixation.

Having a good bone response leads to less risk of implant detachment or loosening. Osseointegration is related to both cell attachment and proliferation, and involves a large number of biological factors. However, the success of bone response in prosthetic implant osseointegration processes largely depends on the surface properties of the applied material.[2] A large body of research has been carried out to improve biological responses of the human body to biomaterials, mainly related to enhancing the adhesion of bone osteoblasts, which are the cells responsible for bone formation, to the implant surface.[2–6]

The development of highly porous surfaces and scaffolds to mimic the so-called trabecular structure of cancellous bone (a network of spongy tissue found, for example, at the core of bones) is of great interest, and its successful application is demonstrated by clinical evidence.[7,8] There is a large body of scientific literature on the ability of natural bone to re-grow within narrow porosities of cellular solids and metal foams, designed to be as close as possible to the trabecular porous structure of natural bone.[3,7,8] All of these efforts have led to the creation of a number of technologies used by the orthopedic implant industry toward the creation of novel porous surfaces to be in contact with bone, such as vacuum plasma spray (VPS), chemical vapor deposition, and low-temperature arc vapor deposition. Despite overall positive clinical outcomes, enhancing implant surface complexity resulted in some drawbacks, such as porous layer detachment from the substrate, corrosion phenomena, and implant loosening.[9–11] This propelled further research seeking the optimal technologies and porous structures to be employed.

Pore size and porosity play critical roles in the formation of new bone tissue. In fact, a minimum pore size of 300 μm appears to be necessary in order to improve osseointegration. Further, it has been found that the growth of osteoblast is quicker in 600 μm diameter holes than other diameters, ranging from 300 to 1000 μm.[7] In addition, bone response can be enhanced by surface roughness as well. It has been demonstrated that microtexturing (10–50 μm) enhances the osseointegration properties of the scaffold, such that comparable levels of bone ingrowth can be obtained even with different pore diameters and porosity.[12,13] It has to be considered, however, that porosity and roughness affect the mechanical

Marco Regis, Lima Corporate, Italy; marco.regis@limacorporate.com
Elia Marin, Chemistry, Physics, and Ambient Department, University of Udine, Italy; elia.marin@uniud.it
Lorenzo Fedrizzi, Chemistry, Physics, and Ambient Department, University of Udine, Italy; lorenzo.fedrizzi@uniud.it
Michele Pressacco, Lima Corporate, Italy; michele.pressacco@limacorporate.com
DOI: 10.1557/mrs.2015.1

© 2015 Materials Research Society

https://doi.org/10.1557/mrs.2015.1 Published online by Cambridge University Press

properties of the realized structures and have to be appropriately designed for mechanical and clinical safety of the overall prosthesis. In this sense, a good combination of mechanical strength, pore shape and dimensions, and elastic modulus, without neglecting biocompatibility and corrosion resistance, are key factors to ensure the success of an implant. Moreover, the manufacturing techniques used to produce such scaffolds and structures are often complex and not scalable at an industrial level.

One of the most promising technologies for efficiently realizing porous scaffolds is electron beam melting (EBM). According to the findings, the desired maximization of bone ingrowth can be efficiently obtained by realizing porous components with this technology.[3,11] The EBM additive manufacturing technique has been extensively studied and applied in the prototyping of a wide range of industrial applications.[14–17] The EBM process conditions allow for the realization of components made of high-melting-point alloys. The advantages of additive manufacturing technology in the production of porous scaffolds are related to high-volume production capacity and process control, as well as to the possibility of easily modifying the geometry of the produced structures, which is based on three-dimensional computer-aided design (3D CAD) models.[18] In the EBM process chamber, under vacuum conditions, the electron beam can melt several high-melting-point alloys, since the temperature reached is approximately 2000°C; for example, 1650°C is the melting temperature of a titanium grade 5 alloy (Ti6Al4V),[19] which is the state-of-the-art material choice for ensuring an optimal implant-bone interaction and, generally, for the whole orthopedic field. With this process, the structure of the cellular solids is mainly influenced by the surface tension of the molten alloy, EBM spot diameter, powder particle diameter, and gravity on the liquid melt pool during melting.[20] The latter depends on the type of liquid that, when standing on powder and not on solid metal, may penetrate into the substrate. All these aspects have to be properly addressed in order to efficiently realize composite scaffolds with the desired materials and properties.

One of the major examples in the production of highly porous orthopedic components is Trabecular Titanium (TT). TT was originally developed to obtain a cellular structure with superior osseointegration properties to be applied on the prosthesis surface, thanks to the promising potential of the EBM additive manufacturing technology. The EBM process creates monoblock components, in which TT is applied to the outer surfaces of acetabular cups (one of the three crucial pieces in hip replacement; the other two pieces are the femoral stem and a head piece) to be implanted in the pelvis during hip joint reconstruction in order to maximize bone response. TT is a porous structure with two mesh sizes, 640 and 1200 μm, both based on multiplanar hexagonal cells, and its morphology and properties have been designed to imitate the natural trabecular bone.[21] The titanium powder beads melt to realize the desired cellular solids, which naturally create roughness at a microscale on the melted arms, and with a 640 or 1200 μm open porosity, both structures ensure high levels of osseointegration.[11,22–24] TT is produced using either titanium grade 5 (Ti6Al4V alloy) or titanium grade 2 (non-alloyed, commercially pure) and is currently applied to acetabular and shoulder prostheses.

The aim of this article is to (1) summarize what has been done regarding the morphological, mechanical, and biological characterization of the EBM manufactured TT structures in order to assess the material performances, and (2) evaluate the overall clinical performance of TT prosthetic implants made with additive manufacturing technology.

TT morphology and structure

The cellular structure of TT has been realized by using 3D CAD modeling software. The unit cell is based on a hexagon developed on three planes, mimicking the diamond crystal structure. Unit cells were replicated in the CAD software and cut according to the desired geometries with Boolean operations. An image of the designed porous structure is depicted in **Figure 1**a. Cylindrical scaffolds were prepared in order to evaluate pore size distribution and, qualitatively, the shape and roughness of the metallic arms. By rotating the samples 45° in both the *xy* and *z* planes, it was possible to expose the hexagonal plane passing through the two opposite vertices and the center of gravity of the cellular element, and to analyze the structure's appearance and porosity.

Figure 1b shows a typical image of the TT scaffold: Pore shape and dimensions are repeated through the entire volume, indicating that the EBM process is able to realize regular and repeatable structures. The metallic surfaces appear pleated and irregular in Figure 1, and hence, a single porosity does not look like a perfect hexagon but rather has a microtextured rough shape. Pore volumes show comparable dimensions. All corners and vertices appear rounded, and a single metallic arm

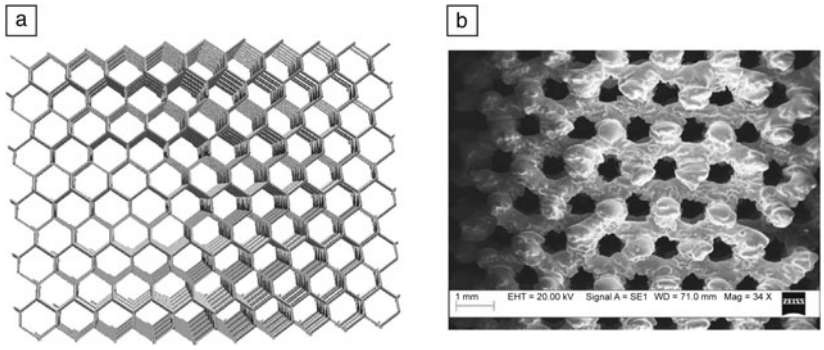


Figure 1. (a) Trabecular Titanium (TT) structure three-dimensional model and (b) scanning electron microscope image of a TT scaffold used to assess pore dimensions and arm thicknesses.

https://doi.org/10.1557/mrs.2015.1 Published online by Cambridge University Press

is thicker than in the CAD file, indicating that the EBM process has a minimum threshold in terms of beam spot diameter and accuracy. Pore size measurements were performed using image post-processing software for microscopes and using scanning electron microscopy (SEM) for image acquisition. Data collected show that the pore dimension is 644 μm, with a very narrow size distribution (measurement deviation within 5%).[22] According to reports in the literature,[6] pore dimension is thus optimal for bone ingrowth. Relative density tests with a standard Archimedes principle kit have been conducted in order to complete the morphological characterization of the TT scaffolds. The kit was slightly modified by adding an insulating shell, obtained by wrapping the scaffold with Parafilm M sheets, to separate porosities from water. Tests were performed using a mean value of 4.43 g/cm^3 for the density of the Ti6A14V alloy, as calculated from measurements by a pycnometer. The calculated relative density of TT scaffolds was 65%. All measurements were comparable and reliable, giving less than a 2% difference in the results.[22]

These results are in accordance with those from literature. EBM technology has been successfully used to obtain structures with porosity from 60% up to 95% by simply changing the geometrical parameters of the single cell.[14] Other materials for osseointegration described in the literature such as those obtained by chemical vapor deposition of tantalum on vitreous carbon skeleton can give up to 80% porosity.[25,26]

Microstructure analysis was conducted using a metallographic microscope. The analyses were performed in the three main directions of the structure, resulting in a fine, well-distributed structure, as shown in **Figure 2**.[22] The Ti6A14V mechanical strength is strongly influenced by the processing history and heat treatments, which have an impact on the alloyed phases, their shape, and size. It is well known that thermal history plays a role in the change of a materials microstructure, specifically on the formation of different crystalline domains, or phases, and in their appearance (shape, dimension). By cooling down Ti6Al4V rapidly, the formation of a fine and dispersed microstructure is observed. Ti6Al4V has two phases, α and β, that are formed during cooling. Acicular or lamellar α is the most common transformation product formed from the β phase during cooling. It is a result of nucleation and growth on crystallographic planes of the prior β matrix, and as the cooling rate increases, the lamellar α phase becomes finer. Precipitation normally occurs on multiple variants or orientations of this family of habit planes. α+β acicular structure is desirable, since it possesses good mechanical properties and ductility. With finer grain dispersion, the mechanical properties are more relevant. This is considered to be an advantage of the α+β acicular structure over other kinds of possible Ti6Al4V configurations.[22] A packet or cluster of acicular α grains aligned in the same orientation is referred to as a colony. The measured mean α lamella thickness found was approximately 500 nm, and the mean colony size was about 5–10 elements, which is a low value when compared to conventional techniques such as casting and wrought alloys of Ti6A14V that usually show greater colony size (30 or more elements) and greater lamellar thickness (up to 1000 nm).[27] When correlating this type of microstructure with properties such as fatigue or fracture toughness, colony size is often regarded as an important microstructural feature, as fatigue crack propagation rate was determined mainly by the colony size.[28,29] Since the process was performed in a vacuum atmos phere, oxygen and nitrogen were not absorbed at the surface, so there was no α case formation.[30]

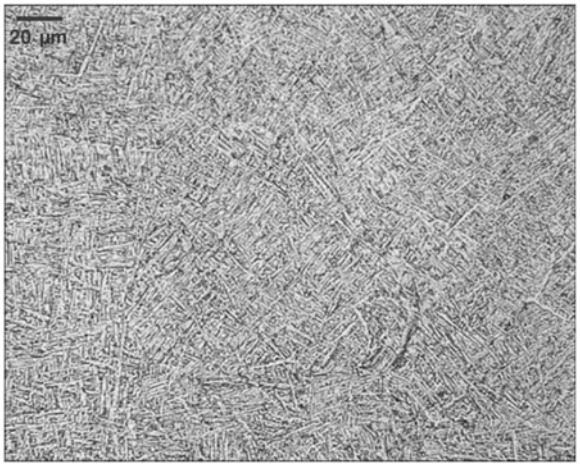


Figure 2. Microstructure of Ti6A14V alloy obtained by electron-beam melting. α (brighter) + β (darker) lamellar structure can be distinguished throughout the whole image. Reprinted with permission from Reference 22. © 2010 Elsevier.

Mechanical properties of TT scaffolds

Tensile and compression tests were performed on TT dog bone shaped (13 × 6.7 mm^2 cross-section and 195 mm length) and cylindrical (10.5 mm diameter and 11.2 mm height) specimens, respectively.[31] Tests were performed at a constant strain rate until breakage of the specimen. Strength was calculated by dividing the applied load with the cross-section of the tested specimens. In addition, the elastic modulus in compression was calculated by extrapolating the angular coefficient of the stress-strain curve within the first 0.2% of deformation, as is typically calculated for metal alloys.

Figure 3 summarizes the mechanical properties of the tested TT specimens.[22] The tensile strength was 40±12 MPa, while the compression resistance was 60±4 MPa. The mechanical behavior was nearly linear up to failure, indicating an elastic response of the structure, with low plastic deformation at high loads, indicating that the structure collapsed rapidly due to progressive breakage of the metallic arms and consequent resistant area reduction. Fracture occurred at 45° inclination, which corresponds to the weakest plane of the TT structure. In contrast, compression tests showed that the TT structure, after the failure of the 45° plane, exhibited a somewhat more complicated behavior, which caused the stress to rise and fall steeply with increasing strain.[32] This was caused by structure

https://doi.org/10.1557/mrs.2015.1 Published online by Cambridge University Press

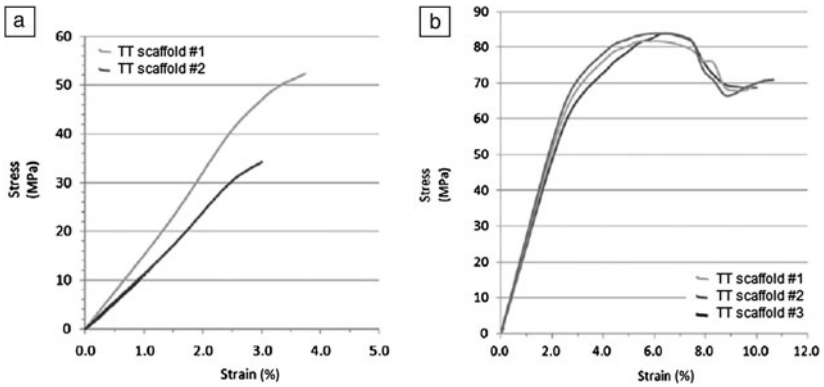


Figure 3. (a) Mechanical behavior in tensile test and (b) compression test for Trabecular Titanium (TT) scaffolds. Reprinted with permission from Reference 22. © 2010 Elsevier.

compaction, which occurs after the slipping of the 45° plane, along which the stress is distributed at the beginning, resulting in the creation of additional resistant planes and leading to compressed structure resistance enhancement and to the possibility for the scaffold to resist at larger strains (**Figure 4**). The calculated compression modulus was 1.12 GPa. Based on values reported in the literature for trabecular bone (5–25 GPa), the compression modulus of TT was close to that of trabecular bone, although the value was lower. This will impact the *in vivo* behavior of the scaffolds, since it is known that bone response is also related to stress shielding effects, which occur due to the non-optimal load transfer from an implanted material or scaffold to the surrounding bone, leading to bone resorption and/or breakage. Having an elastic modulus as close as possible to the surrounding bone would result in an optimal load transfer and, consequently, will eliminate the risk of stress shielding.[33]

Fracture analysis was performed after tensile strength tests. **Figure 5** illustrates the typical site of fracture for a TT metallic arm. In this example, the metallic arm has been ripped off from the node, leaving a curved cup-like fracture surface composed of cavities and division phenomena. On the right side of the node, some neckings can be seen in the picture, and on the left side, the trigger point of another fracture on the same arm. The internal structure of the observed fracture is mainly composed of cavities and division surfaces, and is typical of ductile fracture, in which a structure collapses due to nucleation and growth of microvoids formed on the grain boundary, as soon as the void volumes (interacting with each other) reach critical dimensions.

Additionally, the mechanical resistance of the porous structure was assessed by performing an adhesion test, usually performed to assess the safety of a porous layer on the outer surface of an orthopedic implant. This test was carried out according to the ASTM F1147 standard for coatings, for comparison with previous studies.[22,34] It should be noted that in the present case, the manufacturing technique of the specimens does not produce coated structures but rather a continuous monolithic component. Still, this comparison is useful.

For this purpose, a sandwich-like specimen was prepared, consisting of a bulk/porous layer/bulk structure as illustrated in **Figure 6**a. The test was considered successful if fracture occurred within the porous layer of the sandwich structure, rather than at the interfaces between the bulk and porous layer. Tear-off resistance of the TT structures reached extremely high values, which overcame the actual state-of-the art coating adhesion limits.[35] Adhesion resistance was 86±2 MPa, compared to 50 MPa typically obtained with standard VPS coatings, as shown in Figure 6b.[35] An explanation of this lies in the

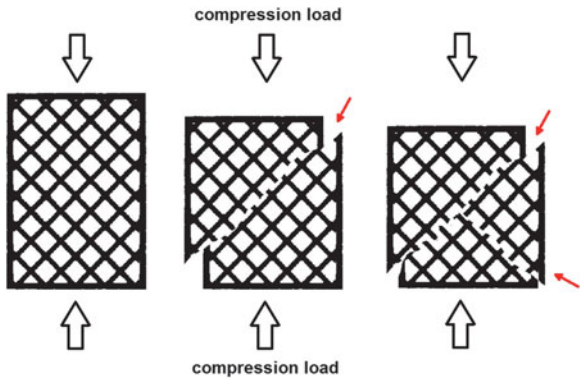


Figure 4. Proposed failure mechanism for Trabecular Titanium scaffolds. From left to right: as the compression force increases, the failure of the 45° plane generates additional resistant planes (indicated by the red arrows) within the scaffold volume, causing an increase-decrease-increase stress trend.

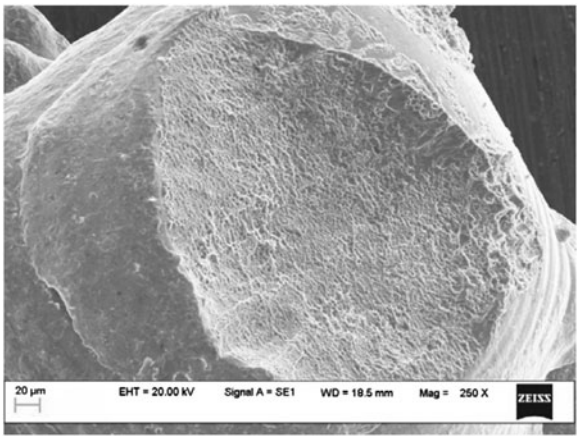


Figure 5. Scanning electron microscope image of an arm fracture of the Trabecular Titanium cellular solid structure highlighting division lines and cavities. Reprinted with permission from Reference 22. © 2010 Elsevier.

https://doi.org/10.1557/mrs.2015.1 Published online by Cambridge University Press

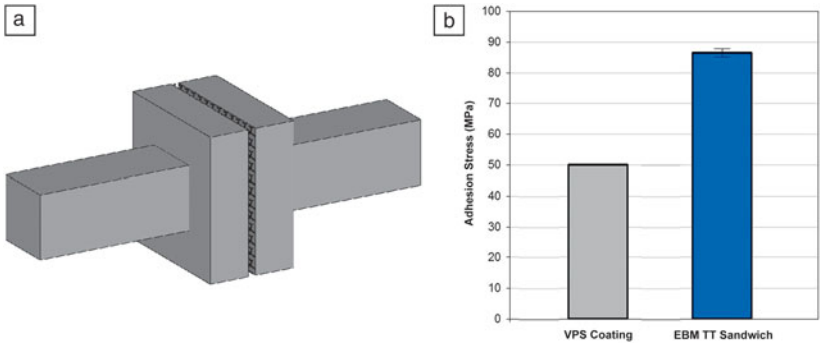


Figure 6. (a) Specimen for the adhesion test. A bulk/porous layer/bulk sandwich specimen was prepared in order to evaluate the tear resistance of the scaffolds against a bulk substrate; and (b) mechanical behavior in adhesion test for Trabecular Titanium (TT) scaffolds, compared to a standard vacuum plasma spray (VPS) coating adhesion resistance. Reprinted with permission from Reference 22. © 2010 Elsevier. Note: EBM, electron-beam melting.

manufacturing technique. EBM is able to produce both the porous structure and the substrate in a single-step process, enhancing the TT scaffold resistance and minimizing the risk of coating detachment.

Biological activity

A detailed characterization of the biological response to the presence of a TT scaffold is essential for determining the prospects of application of the structure and related manufacturing technology to orthopedic prostheses. In fact, the presence of the highly porous structure with appropriate pore size is expected to enhance cell migration and vascularization in the implantation area, facilitating the transport of oxygen, nutrients, and bone-inducing factors that lead to enhanced bone formation.[7,8]

Research has thus far been focused on demonstrating that TT porous scaffolds are able to promote new bone cell formation and stimulate cell proliferation and attachment, as well as cell differentiation into bone tissue. In order to do so, biochemical and morphological methods were used to assess the adhesion and differentiation of human adipose tissue-derived stem cells (hADSCs) grown on TT scaffolds.[36–38] hADSCs share many of the characteristics of their counterpart marrow cells, including extensive proliferative potential and the ability to differentiate into multiple cell typologies.

A first evaluation with hADSCs isolated from subcutaneous adipose tissue was performed by seeding the cells on a monolayer control sample and on TT scaffolds, and by incubating the cultures at 37°C in 5% CO_2 with both an osteogenic medium containing stem cells and a control medium.[36] The results showed that hADSCs were able to adhere to titanium scaffolds, proliferate, acquire an osteoblastic-like phenotype, and produce a calcified extracellular matrix with protein, such as decorin, fibronectin, osteocalcin, osteonectin, osteopontin (proteins that aid in the formation of cellular matrix and specific cell formation), and Type I collagen, which is related to bone matrix (**Figure 7**). The data suggest that this kind of scaffold/cells construct is effective to regenerate damaged tissue and to restore the function of bone tissue.

hADSCs were also used to determine if the beneficial effect of bone matrix formation was induced by any porous structure or specifically in the presence of TT.[37] The hADSCs were isolated from subcutaneous adipose tissue during orthopedic surgery and were used to induce osteogenic differentiation for 28 days on scaffolds of three different synthetic materials, namely polylactide-co-glycolide (PLGA), polylactide-co-glycolide/hydroxyapatite (PLGA/HA), and TT scaffolds (Ti6A14V). PLGA and PLGA/HA are commonly used to fabricate scaffolds for tissue regeneration, and their performance was compared with that of TT structures. Osteogenesis was assessed by enzyme-linked immunosorbent assay quantification of extracellular matrix protein expression, von Kossa staining to determine cell mineralization via precipitation reaction, x-ray microanalysis, and SEM. A higher amount of protein matrix on the TT scaffold with respect to PLGA and PLGA/HA was observed. Further, SEM images showed that cell growth and mineral bone matrix deposition on the TT scaffolds was extensive (**Figure 8**). The scaffold is entirely covered by mineralized bone, creating the bone matrix within the scaffold porosity to the point that the metallic structure is fully covered and cannot be detected.[36] These lead to the conclusion that TT scaffolds significantly affect cell proliferation.[37]

Another *in vitro* study was designed to thoroughly investigate the mechanism of interaction between TT and osteoblasts.[38] To do so, genetic evaluation of the effects of TT on osteoblast-like cells (MG63) in a cell line culture was performed by using DNA microarrays technology, which

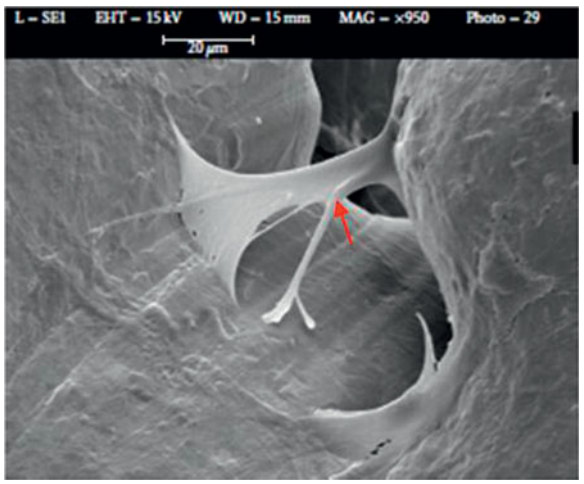


Figure 7. Human adipose stem cells adhesion (indicated by the red arrow) on Trabecular Titanium scaffolds. Reprinted with permission from Reference 37. © 2010 Hindawi.

https://doi.org/10.1557/mrs.2015.1 Published online by Cambridge University Press

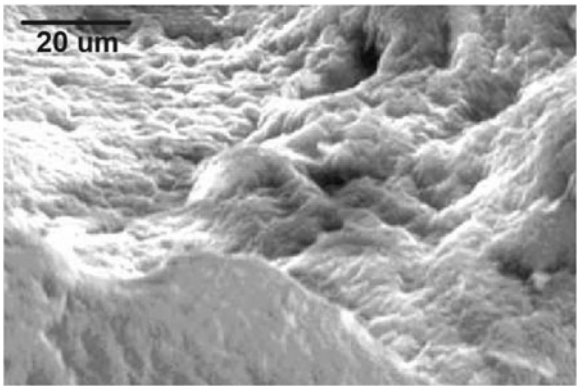


Figure 8. Cell proliferation and differentiation into osteoblastic cells with deposition of calcified bone matrix on Trabecular Titanium scaffolds. The scaffold is entirely covered by mineralized bone, creating the bone matrix within the scaffold porosity to the point that the metallic structure is fully covered and cannot be detected. Reprinted with permission from Reference 36. © 2010 Wiley.

provides the ability to comparatively analyze mRNA expression of thousands of genes in parallel. In this way, it was possible to show that the MG63 activated and repressed genes in the presence of the TT scaffold. Osteoblast-like cells were cultured in Eagle's minimal essential medium, supplemented with 10% fetal bovine serum and antibiotics, and maintained in a 5% CO_2 humidified atmosphere at 37°C. Cells were then collected, seeded, and, after 24 hours, processed for RNA extraction. Genetic expression was quantified using real time reverse transcription polymerase chain reaction to amplify the genetic signal. It was seen that several genes were significantly up- or down-regulated by the presence of the TT scaffold. TT increases the transcription of some mRNAs, which enhances osteoblast activity while reducing inflammation and immunologic events. No major adverse effects of TT on cells were detected. Globally, it can be stated that TT stimulates osteoblast proliferation and differentiation, and reduces apoptosis (natural process of programmed cell death).[38]

All these effects can contribute toward improving the osseointegration of TT. The data reported overall encouraged the clinical application of TT to prosthetic devices.

Clinical performance of TT acetabular components

TT prostheses have been cleared for clinical use by the European Union and the United States regulatory authorities and have been consequently launched in the market since 2007. After their commercialization, a number of studies have been conducted to assess the clinical success of the EBM-made TT acetabular shells. As in the case of every non-cemented porous cup used in orthopedic prostheses, initial mechanical fixation and surface texturing (porosity of the outer surface) are crucial for implant fixation and surrounding bone remodeling. These aspects have been evaluated by follow-up with regard to both clinical and radiographical evaluations. Another important indicator for implant success is the so-called Harris Hip Score (HHS), which is calculated by evaluating the recovery of the patient after surgery in terms of daily activities and range of motion of the treated limb. Three main studies were carried out for the TT acetabular shells, two concerning primary surgery, and one concerning revision surgery.[39–41] Thus, two versions of the shells were considered, according to the surgical intervention needed, named Delta TT and Delta Revision TT, respectively (**Figure 9**).

Between December 2007 and January 2011, 94 consecutive patients (not selected for any specific pathologies, for a total of 103 hips treated) underwent primary total hip arthroplasty with the Delta TT cup, without restrictions or limitations derived from patient condition or pathologies.[39] The mean patient age was 66.8±14.1 (37–85) years. The underlying pathology was primary osteoarthritis in 88 cases (85.4%), hip dysplasia (hip joint misalignment) in 10 cases (9.7%), osteonecrosis of the femoral head (bone collapse due to poor blood vascularization) in four cases (3.9%), and rheumatoid arthritis in one case (1%). Clinical and radiographic evaluations were performed in the preoperative phase and postoperatively at three, six, and 12 months, and annually thereafter. Average follow-up was 35.4±4.2 (28–41) months. The mean total HHS improved considerably from 53.9±7.5, before surgery, to 93.1±7.8 at the last follow-up. A significant improvement was observed in terms of functional recovery and pain relief: All patients regained a normal lifestyle without limitations.

Radiographic assessment indicated that the acetabular cups showed signs of osseointegration without osteolysis or

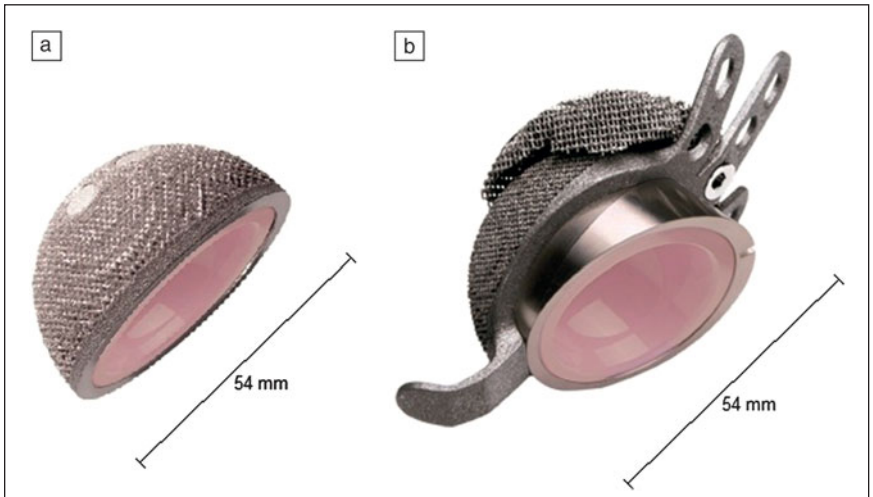


Figure 9. (a) Delta Trabecular Titanium (TT) acetabular cup and (b) Delta TT Revision cup. Both products are made by the electron-beam melting process with a monoblock TT layer on the outer surface to improve implant osseointegration.

https://doi.org/10.1557/mrs.2015.1 Published online by Cambridge University Press

progressive radiolucent lines, indicating the absence of bone resorption or fibrous tissue growth, respectively. Kaplan-Meier cumulative survivorship, used to estimate the number of survived implants on the total number of implanted prostheses after the considered period, was 99.08%. Only one revision (0.9%) due to aseptic loosening was recorded after 11 months. In a similar study completed between 2008 and 2011, 109 Delta TT cups were implanted in 98 patients, 65 males and 43 females, with an average age of 63 and 65 years, respectively, at the time of surgery.[40] The acetabular component was coupled to different types of stems. All patients were evaluated both radiographically and clinically with the HHS at the pre-operative examination, at three months and six months after surgery and then yearly. The mean follow-up was 15 months (minimum two months and maximum 36 months). The total mean HHS value and all specific domains significantly improved from pre-operative evaluation to the last follow-up. X-ray evaluation revealed no signs of loosening or migration of the cups, nor periacetabular signs of osteolysis. The inclination angle of the implanted cup was within the physiological range of 40±5° of coverage in all cases, indicating that no cup micro-movement or misalignment occurred during the surgical procedure or later.

Clinical and radiographic results of 31 cases of acetabular revisions with the Delta TT Revision shell, performed from June 2007 to March 2012, were also prospectively assessed.[41] The mean age of patients was 69.5 years (range 29–90). The revision causes were aseptic loosening in 22 cases (71.0%), periprosthetic acetabular fractures in four cases (13.0%), multiple dislocation of the primary implant in three cases (9.6%), and outcome of infection in two cases (6.4%). The average follow-up was 32 months (range 12–69). The mean HHS significantly increased from 39.9 (range 17–60) preoperatively to 86.5 (range 65–100) at the last follow-up examination. The implanted cups were radiographically stable at the last follow-up visit without radiolucent lines or periprosthetic osteolysis. No major complications were observed.

In all studies, the TT cups showed promising short-term clinical and radiographic results (**Figure 10**), ensuring effective primary fixation and osseointegration. All patients presented satisfactory clinical outcomes, and none complained of persistent pain or any other discomfort related to the prosthetic implant. TT showed a high capacity of osseointegration, providing excellent results in short to midterm follow-up.



Figure 10. X-ray image of an implanted Delta Trabecular Titanium acetabular cup. Reprinted with permission from Reference 40. © 2011 Springer.

Summary

Results obtained through research on TT scaffolds and the great amount of data have clearly demonstrated that EBM technology can efficiently be employed for the production of implantable prostheses with enhanced bone fixation and biocompatibility, with incredibly higher degrees of freedom concerning geometries and manufacture of porous structures.

Supported by the promising results, new applications of the TT structure have been released, such as a shoulder prosthesis glenoid component named Metal Back TT, with the aim to extend the use of EBM technology and TT structure to a larger number of different bone replacement applications. This leads to new possibilities in orthopedics and the ability to foresee great improvements in the patients' quality of life.

References

1. R.J. Friedman, J. Black, J.O. Galante, J.J. Jacobs, H.B. Skinner, *J. Bone Joint Surg. Am.* **75** (7), 1086 (1993).
2. K. Anselme, *Biomaterials* **21** (7), 667 (2000).
3. P. Heinl, L. Muller, C. Korner, R.F. Singer, F.A. Muller, *Acta Biomater.* **4** (5), 1536 (2008).
4. M. Baleani, M. Viceconti, A. Toni, *Artif. Organs* **24** (4), 296 (2000).
5. A. Christensen, A. Lippincott, R. Kircher, *Proc. Conf. MEDDEV*, Palm Desert, 2007, (ASM International ed., Materials Park, OH) p. 129.
6. V.M. Goldberg, *Clin. Orthop. Relat. Res.* **319**, 122 (1995).
7. K.H. Frosch, F. Barvencik, V. Viereck, C.H. Lohmann, K. Dresing, J. Breme, E. Brunner, K.M. Sturmen, *J. Biomed. Mater. Res.* **68A** (2), 325 (2004).
8. V. Karageorgiou, D. Kaplan, *Biomaterials* **26**, 2775 (2005).
9. S.D. Cook, K.A. Thomas, J.F. Kay, *Clin. Orthop.* **265**, 280 (1991).
10. X. Li, C. Wang, W. Zhang, Y. Li, *Mater. Lett.* **63** (3–4), 403 (2009).
11. P.M. Bonutti, R. Pivec, K. Issa, B.H. Kapadia, S. Banerjee, S.F. Harwin, M.A. Mont, T.W. Bauer, *Orthopedics* **36** (8), 417 (2013).
12. H.R. Bloch, S. Burelli, D. Devine, D. Arens, *Proc. Conf. 13th EFORT*, (Berlin, 2012), p. 85.
13. M. Mour, D. Das, T. Winkler, E. Hoenig, G. Mielke, M.M. Morlock, A.F. Schilling, *Appl. Mater.* **3**, 2947 (2010).
14. O. Cansizoglu, D. Harrysson, D. Cormier, H. West, T. Mahale, *Mater. Sci. Eng.* **492** (1–2), 468 (2008).
15. J.C.S. Pires, A.F.B. Braga, P.R. Mei, *Sol. Energy Mater. Sol. Cells* **79** (3), 347 (2003).
16. A. Hershcovitch, *Nucl. Instrum. Methods Phys. Res. B* **241** (1–4), 854 (2005).
17. Q.F. Guan, H. Zou, A.M. Wu, S.Z. Hao, J.X. Zou, Y. Qin, C. Dong, Q.Y. Zhang, *Surf. Coat. Technol.* **196** (1–3), 145 (2005).
18. S. Kalpakjian, S.R. Schmid, *Manufacturing Engineering and Technology* (Prentice Hall, Upper Saddle River, NJ, 2009).
19. M. Niinomi, *Mater. Sci. Eng.* **243** (1–2), 231 (1998).
20. S. Schneider, I. Egry, I. Seyhan, *Int. J. Thermophys.* **23** (5), 1241 (2002).
21. P. Dalla Pria, M. Pressacco, E. Veronesi, *Sphera Med. J.* **7**, 4 (2008).
22. E. Marin, S. Fusi, M. Pressacco, L. Paussa, L. Fedrizzi, *J. Mech. Behav. Biomed. Mater.* **3** (5), 790 (2010).
23. E. Marin, M. Pressacco, S. Fusi, A. Lanzutti, S. Turchet, L. Fedrizzi, *Mater. Sci. Eng. C* **33**, 2648 (2013).
24. D. Devine, D. Arens, S. Burelli, H.R. Bloch, L. Boure, *J. Bone Joint Surg.* **94B**, 201 (2010).

https://doi.org/10.1557/mrs.2015.1 Published online by Cambridge University Press

25. B.R. Levine, S. Sporer, R.A. Poggie, C.J. Della Valle, J.J. Jacobs, *Biomaterials* **27** (27), 4671 (2006).
26. L.D. Zardiackas, D.E. Parsell, L.D. Dillon, D.W. Mitchell, L.A. Nunnery, R. Poggie, *J. Biomed. Mater. Res.* **58** (2), 180 (2001).
27. R.R. Boyer, *Metals Handbook* 9th ed. (ASM International, Materials Park, OH, 1985).
28. G.R. Yoder, L.A. Cooley, T.W. Crooker, *Eng. Fract. Mech.* **11** (4), 805 (1979).
29. G.R. Yoder, D. Eylon, *Metall. Mater. Trans. A* **10**, 1808 (1979).
30. S.Y. Sung, Y.J. Kim, *Mater. Sci. Eng. A* **405** (1–2), 173 (2005).
31. ISO 13314, *International Standardization Organization*, 2011.
32. M.F. Ashby, A. Evans, N.A. Fleck, L.J. Gibson, J.W. Hutchinson, H.N.G. Wadley, *Metal Foams—A Design Guide* (Butterworth-Heinemann, Oxford, UK, 2000).
33. J.J. Callaghan, A.G. Rosenberg, H.E. Rubash, in *The Adult Hip* 2nd ed. (Lippincott Williams & Wilkins, Philadelphia, PA, 2007), vol. 1.
34. ASTM F1147, *ASTM International*, 2005.
35. L. Gilmour, B. Jones, J. Dickinson, *Proc. Conf. MEDDEV*, Memphis, 2009, (ASM International ed., Materials Park, OH), pp. 129–132.
36. G. Gastaldi, A. Asti, M.F. Scaffino, L. Visai, E. Saino, A.M. Cometa, F. Benazzo, *J. Biomed. Mater. Res. A* **94** (3), 790 (2010).
37. A. Asti, G. Gastaldi, R. Dorati, E. Saino, B. Conti, L. Visai, F. Benazzo, *Bioinorg. Chem. Appl.* **83**, 176 (2010).
38. V. Sollazzo, A. Plamieri, L. Massari, F. Clarinci, *J. Orthop. Traumatol.* **13** (1), 107 (2012).
39. A. Bistolfi, L. Ravera, E. Graziano, G. Collo, D. Malino, A. Giordano, G. Massazza, *Minerva Orthop. Traumatol.* **65**, 199 (2014).
40. L. Perticarini, L. Piovani, S.M.P. Rossi, A. Combi, A. Padolino, F. Benazzo, *J. Orthop. Traumatol.* **12** (Suppl. 1), 147 (2011).
41. L. Perticarini, M. Ghiara, T. Lamberti, F.M. Benazzo, *Bone Joint J.* **95B** (Suppl. 34), 479 (2013). □





https://doi.org/10.1557/mrs.2015.1 Published online by Cambridge University Press